Supporting Information

Rapid Monitoring of Graphene Exfoliation Using NMR Proton Relaxation

Sofia Marchesini‡, Piers Turner‡, Keith R Paton, Benjamen P Reed, and Andrew J Pollard*

* Corresponding Author: andrew.pollard@npl.co.uk, +44 (0) 89436266

National Physical Laboratory, Hampton Road, Teddington, TW11 0LW, UK

Materials – Exfoliation of graphite using a sonoreactor
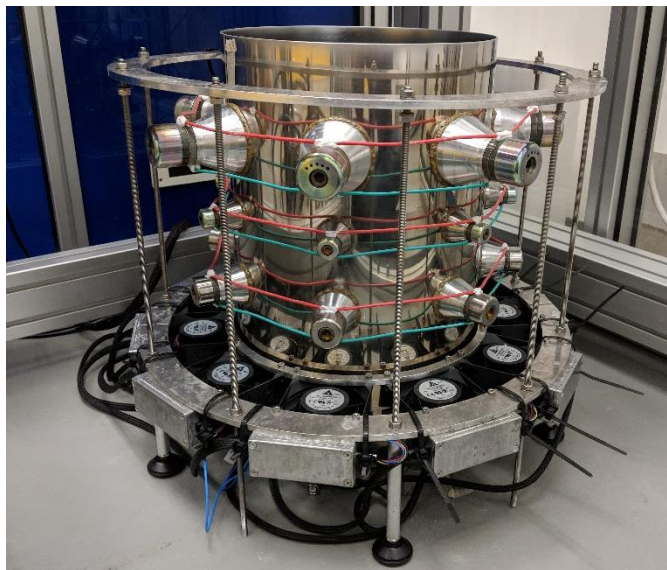

Figure S1. Photograph of the National Physical Laboratory's 17-litre multi-frequency reference cavitating vessel with transducers around the circumference, referred to as the sonoreactor.

Scanning Electron Microscopy:
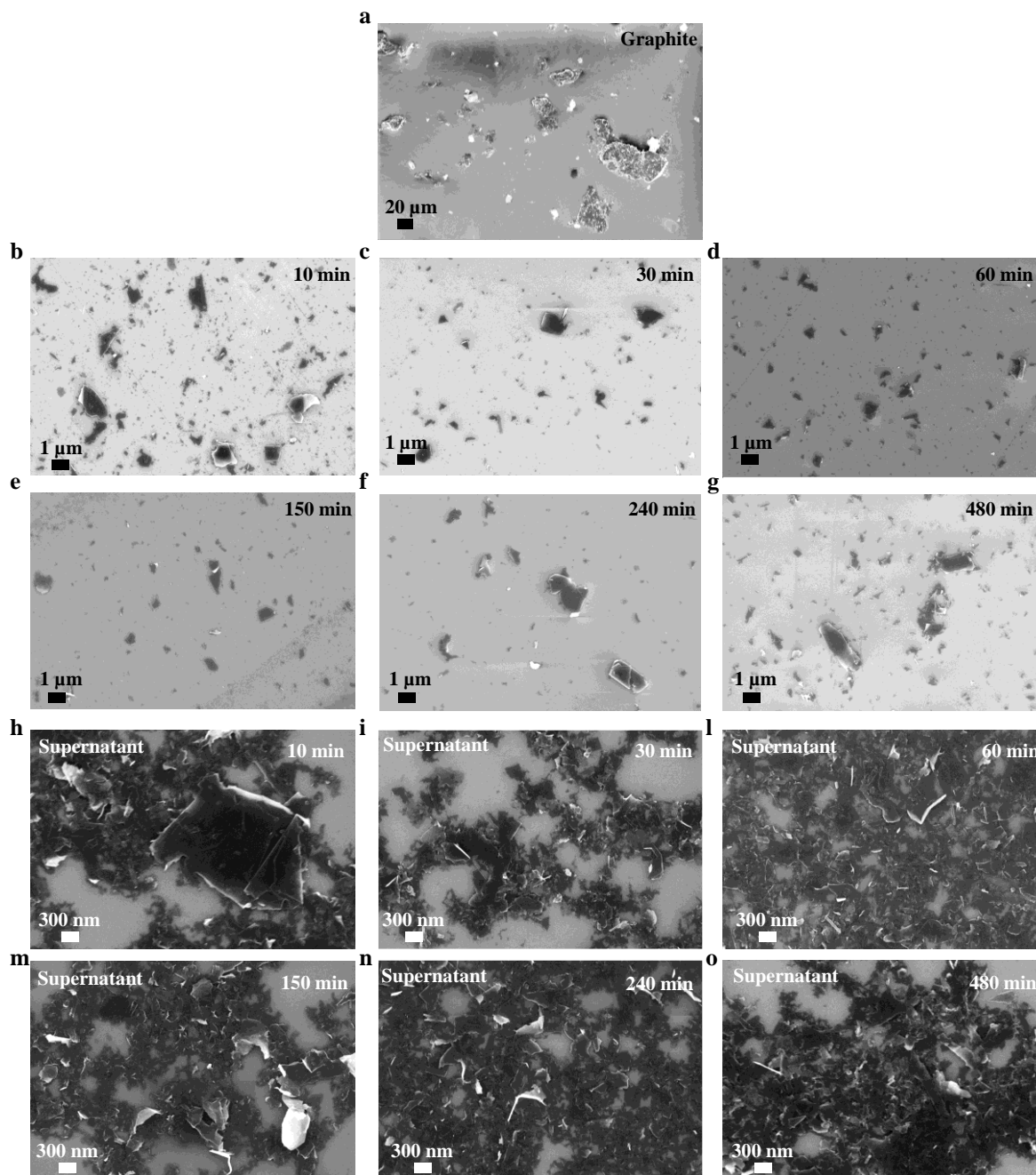
Additional representative images

Figure S2. Representative SEM images for: a) as-received graphite, scale bar represents 20 µm; b-g) Exfoliated dispersions, scale bars represent 1 µm, h-o) Particles deposited from supernatant of exfoliated dispersions centrifuged at 250 g for 2 h, scale bars represent 300 nm.

Laser diffraction:

Table S1. Table of parameters used for Laser diffraction

Beam Length (mm)	2.5
Alignment Type	Automatic
Analysis Model	General Purpose
Scattering Model	Mie
Is Particle Fraunhofer?	No
Particle Refractive Index	2.4105
Particle Refractive Index Blue	2.4334
Dispersant Refractive Index	1.4790
Laser Power (%)	80.75 – 81.54
Laser Obscuration (%)	9.95 – 14.77
Obscuration Low Limit (%)	0.01
Obscuration High Limit (%)	50
Stirrer Speed Achieved (rpm)	1000 – 1500
Weighted Residual (%)	0.19 – 0.80
Residual (%)	0.19 – 0.79
Excluded Inner Detectors	None

Data analysis

The "apparent diameters" of the particle populations were calculated from Figure 1b, as the X-values ("apparent diameter") at which the distribution exhibit local maximum. The apparent diameters of the modes for the most prominent peaks (1 or 2 peaks with highest intensity) from Figure 1b are reported in Figure S3a against the duration of the sonication on a square root axis (error bars represent standard deviations between 5 repeats). Results were generally highly repeatable, as shown by the small error bars in Figure S3a, except for the smaller peak in the sample sonicated for 5 min due to the uncertainty resulting from peak deconvolution. Figure S3a shows two main populations of particles, both linearly decreasing in size with the square root of sonication time, which is consistent with previous findings.[1] The apparent diameter of the largest population (in black, apparent diameter > 100 µm) have a size that is consistent with the starting graphite material. These large particles were seen in SEM images of the starting graphite, but not the sonicated samples. As this population disappears within the first 5 minutes of sonication, this demonstrates that larger particles are preferentially fractured/exfoliated during sonication.[1] Particle populations < 100 µm (in red) are likely to be particles that have been fractured from the initial graphite particles by inertial cavitation; some graphite particles of this scale were also present in the starting graphite. These particles continually decrease in size as a function of sonication time due to multiplicative stochastic fracturing events.[2]

The sample sonicated for 480 min appeared to have a population of very small (observed as < 0.1 µm in size by laser diffraction) flakes that were not present in other samples. To investigate whether this was a measurement artefact, all the samples were centrifuged at a low speed (250 g) to remove the larger graphitic flakes prior to laser diffraction. After centrifugation, laser diffraction measurements were repeated on the supernatants and showed that all the samples had a similar population of flakes

with apparent diameter below 1 μm (Figure S3b). It is worth noting that the laser diffraction measurements were not very repeatable for the centrifuged samples.
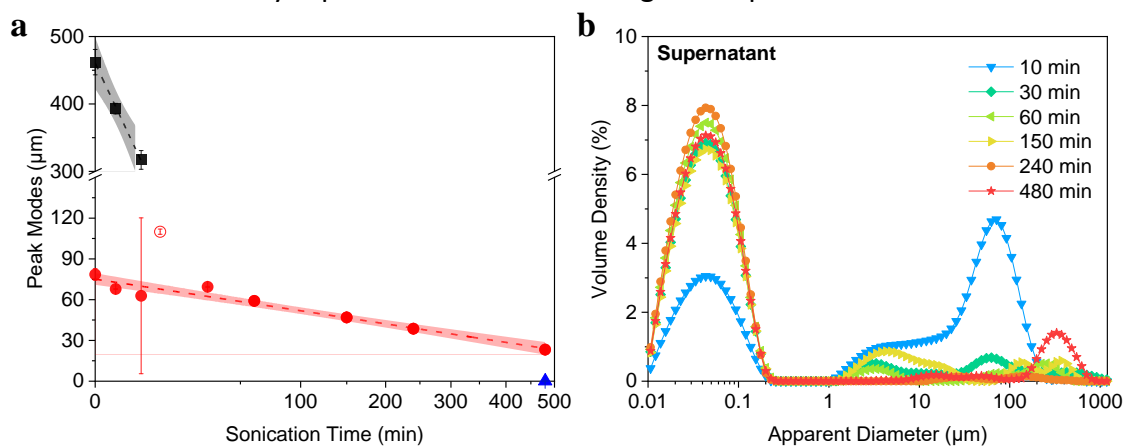

Figure S3. a) Apparent diameters of peak modes from Figure 1b plotted against the duration of the sonication (X-axis is square-root scale), b) Volume-density size distributions of the supernatant solutions from samples sonicated between 10 min and 480 min and then centrifuged at 250 g for 2 h.

UV-Vis spectroscopy:

Results

Figure S4a shows photographs of the supernatants of the centrifuged samples after dilution, with samples exhibiting a darker colour with increasing sonication duration. Figure S4b shows the measured extinction spectra of the supernatant dispersions, after subtraction of the NMP spectrum.
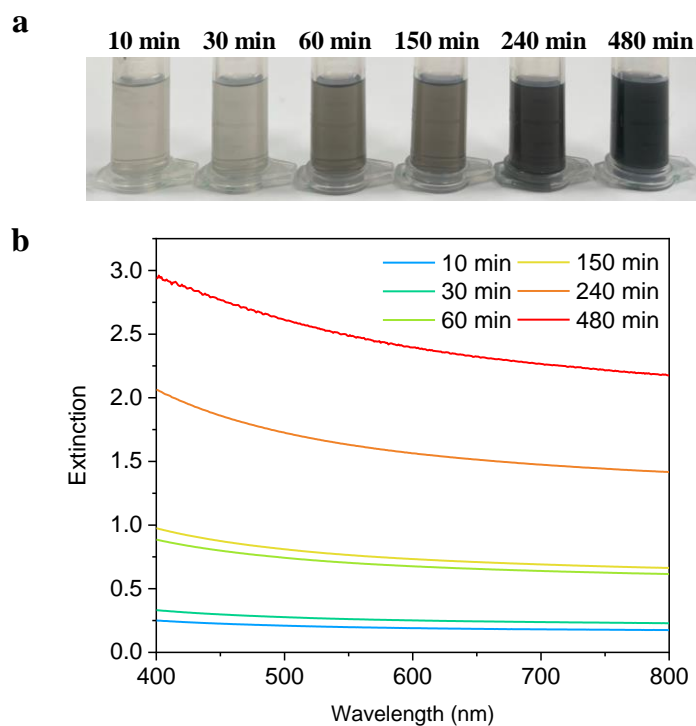

Figure S4. a) Supernatant from exfoliated graphitic dispersions (starting concentrations ~ 20 mg/mL) centrifuged at 250 g for 2 hours and diluted 1:10 v/v; b) Representative extinction spectra of supernatant solutions.

Raman spectroscopy: <u>Data analysis</u>

Before being processed/fitted a relative intensity correction was applied to each spectrum in the Raman map. This relative intensity correction was carried by using a traceably calibrated Standard Reference Material, SRM, (2242a) which consists of a manganese-doped borate matrix glass that has a known relative irradiance at 532 nm; certified by the National Institute of Standards and Technology (NIST). SRMs are secondary emissions standards that are luminescent with laser irradiation, and this luminescence can be calibrated against primary light source standards to provide a source of known relative irradiance.

Prior to fitting, signal artefacts due to cosmic rays were removed by using the method outlined in Whitaker *et al.*[3], a fixed-point baseline (linear interpolation) was subtracted from the spectra, and the spectra were normalised to the G-peak. During fitting, each peak (D, G, 2D) was first isolated from the rest of the spectrum with a Raman shift range 100 cm^{-1} about the approximate centre of the peak and then fitted independently. These peak fitting windows, referred to as "Isolated Peak Range" are also shown in Table S2. The spectra were fitted with a Lorentzian fit function (Equation S1) using the least squares fitting algorithm from the Scientific Python library (SciPy 1.6.0). The fitting bounds are shown in Table S2.

$$y = y_0 + \frac{2A}{\pi} \frac{w}{4(x - x_c)^2 + w^2} \tag{S1}$$

Where y_0 is the offset, A is the area, w is the width and x_c is the centre. Despite using the Renishaw Qontor inVia's LiveTrack feature to maintain an optimal optical focus when measuring large area Raman maps, there were many spectra in which the peaks were not distinguishable from the background noise. This was due to the significant height variations caused by the larger graphite particles in the sample. To ensure the Raman statistics were not skewed by these optical focus challenges, any spectra where the absolute G peak intensity was less than 3× the intensity of the background were discarded. Furthermore, any spectra where the Raman G and 2D peak fit metrics (Width, Area, Centre) were equal to the peak fit bounds were also discarded, as this also suggested the peaks were not distinguishable from the background noise. This filtering procedure reduced the absolute number of Raman spectra in each map, where the minimum number of spectra was 332 for the 10 min sample.

Table S2 The Lorentzian peak fit bounds used to fit all Raman spectra in the study.

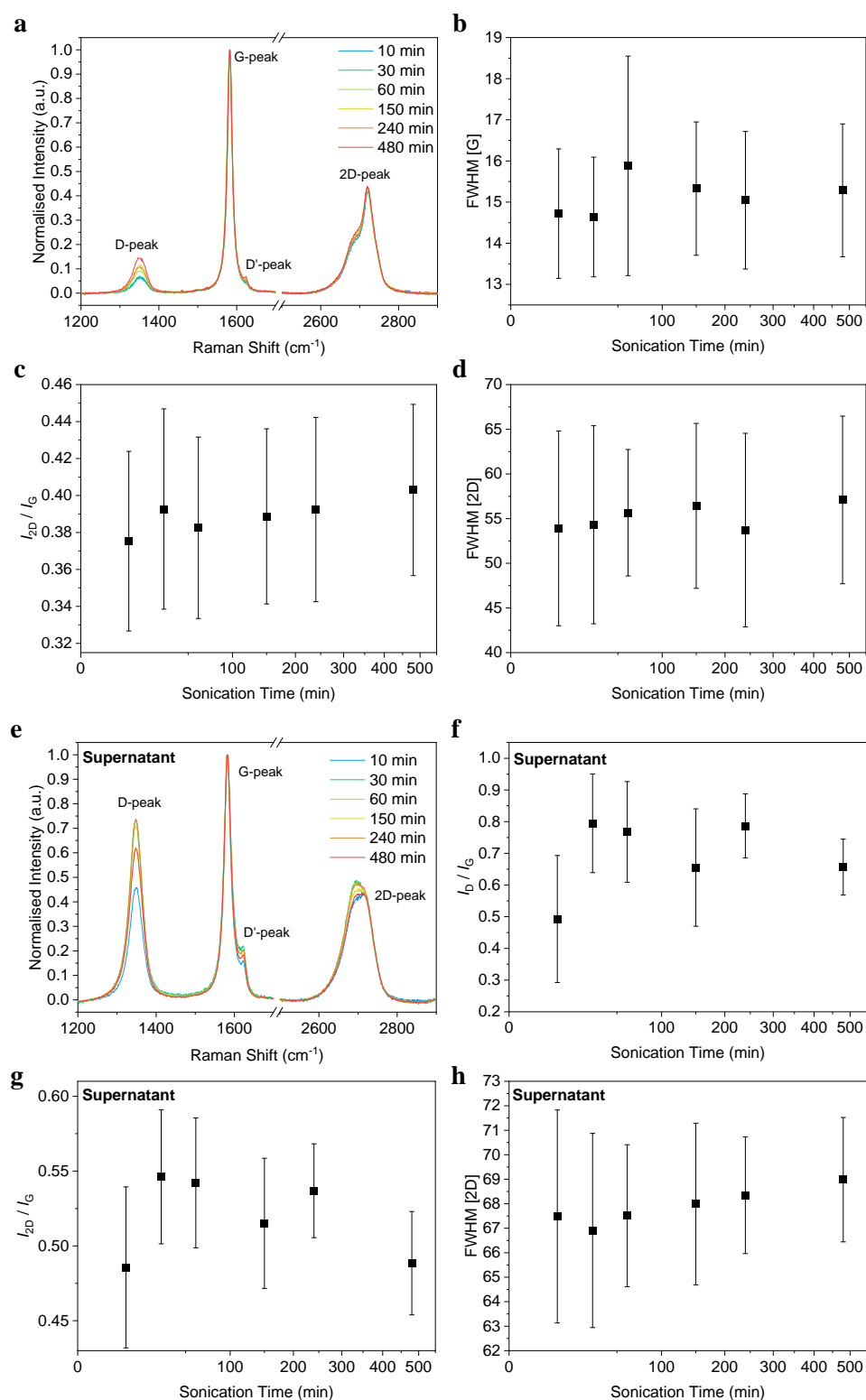| Peak	Fit Metric	Lower Bound (cm^{-1})	Upper Bound (cm^{-1})
D	Isolated Peak Range	1250	1450
	Peak Centre (XC)	1250	1450
	Peak Width (FWHM)	1	100
	Peak Area (A)	1	100
G	Isolated Peak Range	1480	1680
	Peak Centre (XC)	1480	1680
	Peak Width (FWHM)	1	100
	Peak Area (A)	1	100
2D	Isolated Peak Range	2600	2800
	Peak Centre (XC)	2600	2800
	Peak Width (FWHM)	1	100
	Peak Area (A)	1	100

Figure S5. a) Average Raman spectra for all samples, normalised to the intensity of the G-peak; b-d) Raman metrics plotted against the sonication time (square root scale): b) full-width-at-half-maximum (FWHM) of the G-peak, c) I_{2D}/I_G, d) FWHM[2D]; e) Average Raman spectra from supernatant collected after centrifugation at 250 g, normalised to the intensity of the G-peak; f-h) Raman metrics for supernatant plotted against the sonication time (square root scale): f) I_D/I_G, g) I_{2D}/I_G, h) FWHM[2D].

NMR proton relaxation: Methods

The T2 CPMG sequence employs a 90° pulse (6.78 μs) followed by a series of 180° pulses (13.56 μs). The time between the initial 90° and 180° pulse is termed τ, and 180° pulses are repeated every 2* τ. A τ of 0.5 ms has been employed for all measurements. An echo occurs following each 180° pulse until the signal decays. The average peak value of each echo is then plotted as a function of time. A scan is an application of this sequence of pulses. The number of echo cycles for each scan is calculated automatically from the software algorithm so that the total duration of the scan is 5 × T2. The measurement scans are averaged to calculate $M_{xy}(t)$, which is fitted to a single exponential with an offset to calculate T2 (example seen in Figure S6). A total of 4 scans were averaged in each experiment, as no significant effect on the resulting T2 values was observed as the number of scans was increased from 4 to a total of 15 scans. The recycle delay between each scan was set to 5 × T2. The measurement parameters were selected based on a chosen T2 value, which was first estimated by the user and then corrected based on the subsequent measurement result. Measurements were repeated until the initially chosen T2 values were within 20% of the measured values.

The measurement was performed in triplicate and the results averaged. The uncertainty was calculated for a coverage factor k=3. Samples were agitated in between each repeat to minimise any effect due to settling.[4]
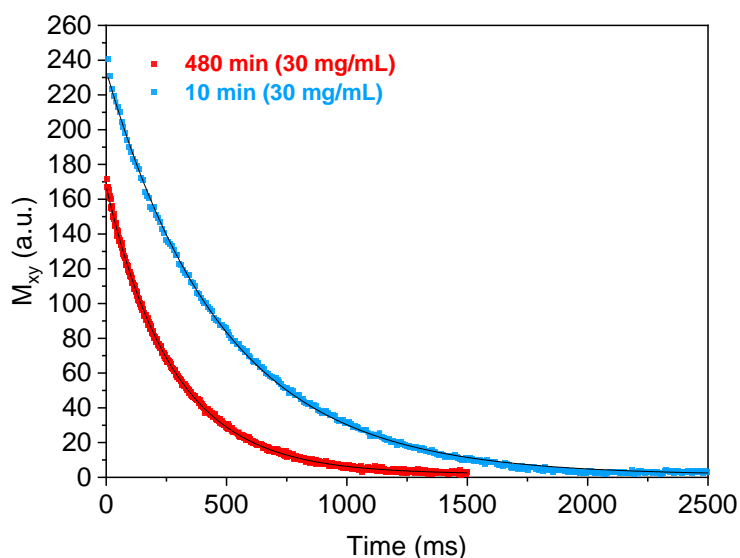

Figure S6. Magnetisation decay curves for dispersions with a concentration of ~30 mg/mL sonicated for 10 min (longest T2 relaxation time) and 480 min (shortest T2 relaxation time) fitted to a single exponential decay with offset ($R^2 > 0.999$).

Gas physisorption analysis: <u>Isotherms</u>

Krypton sorption isotherms collected at 77 K are shown in Figure S7. The isotherms were used to calculate BET SSA values for dry samples reported in the main manuscript.
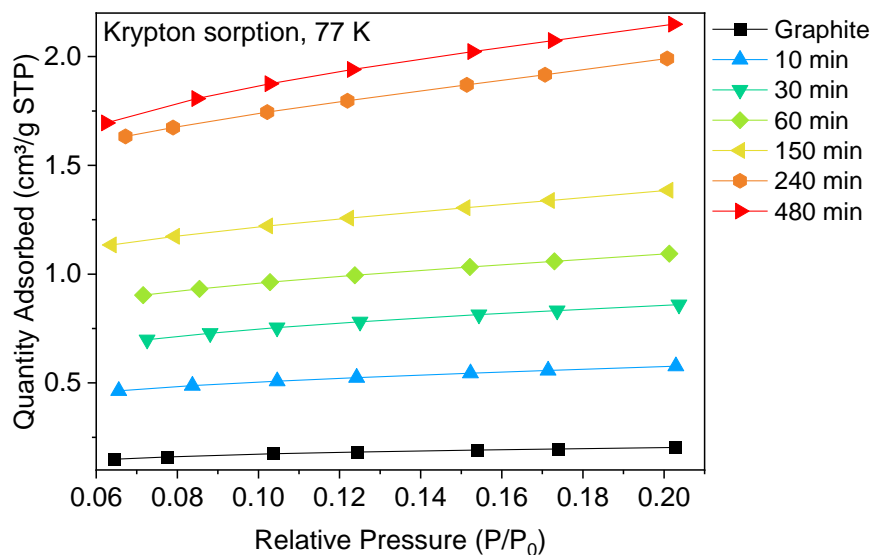

Figure S7. a) Krypton adsorption isotherms at 77 K. Samples sonicated for 1 minute and 5 minutes were not analysed as the dispersions were not stable, making it difficult to collect a representative aliquot for drying. Graphite powder was analysed as received, without dispersion in NMP.

NMR proton relaxation *vs* BET measurements: <u>Results and Discussion</u>

In Figure S8a, K_a values were calculated assuming S equal to BET SSA. This calculation was performed by deriving the volume ratio (Ψ) of dispersions from the mass ratio (Table S3), assuming the density of the solvent (NMP) to be 1.03 g/cm^3 and the density of the particles to be 2.2 g/cm^3, the same as graphite. However, we believe that the assumption of the value of S measured using NMR proton relaxation being equal to BET SSA is actually incorrect, due to aggregation likely occurring during solvent evaporation in samples produced using LPE and then measured with BET.

In Figure S8b,c, S values were calculated by assuming a K_a value of either 0.0021 $\cdot 10^{-3}$ g m^{-2} s^{-1} or 0.0009 $\cdot 10^{-3}$ g m^{-2} s^{-1}.[4] Resulting values of S are much larger than the measured BET SSA values, ranging from ~50 m^2/g to ~260 m^2/g.
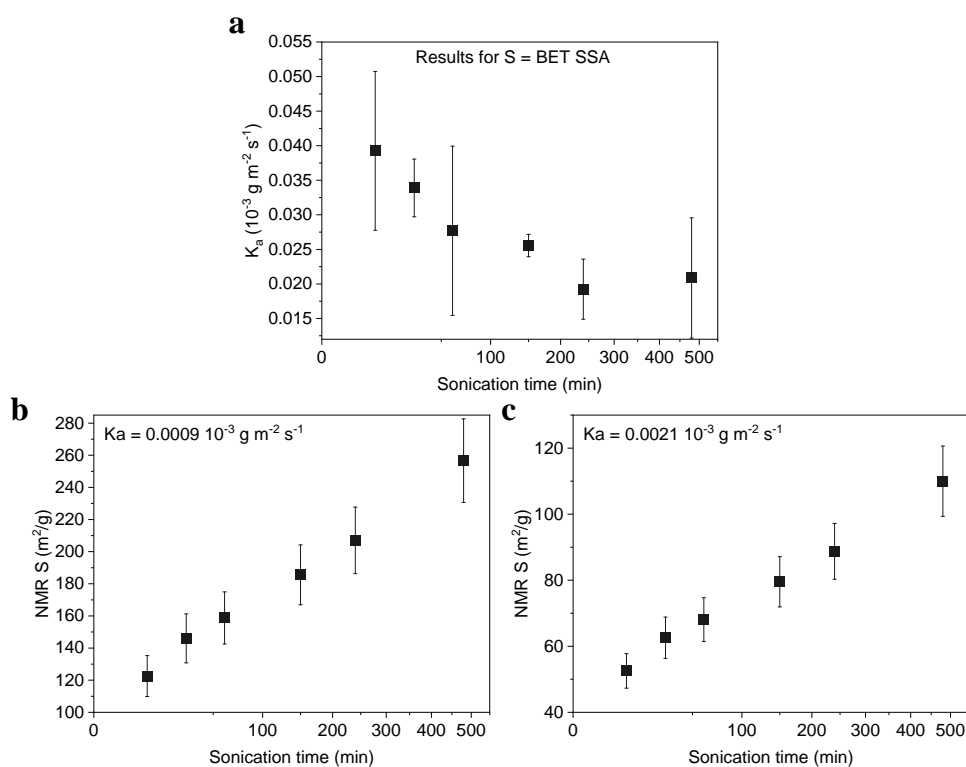

Figure S8. a) Absolute K_a values calculated assuming S equal to BET SSA and constant densities; b, c) NMR S values calculated for constant K_a values and constant densities: b) K_a = 0.0009 $\cdot 10^{-3}$ g m^{-2} s^{-1} and c) K_a = 0.0021 $\cdot 10^{-3}$ g m^{-2} s^{-1}. The sonication time (x-axis) is plotted on a square root scale.

Table S3. Gradients of linear correlations from NMR proton relaxation results.

Sample name	Gradient (R_{av} vs weight ratio) (10^{-3} s^{-1})	Gradient (R_{av} vs Ψ) = SK_a (10^{-3} s^{-1})
10 min	0.052 ± 0.005	0.110 ± 0.010
30 min	0.062 ± 0.005	0.131 ± 0.011
60 min	0.067 ± 0.004	0.143 ± 0.009
150 min	0.078 ± 0.003	0.167 ± 0.006
240 min	0.087 ± 0.001	0.186 ± 0.001
480 min	0.108 ± 0.006	0.231 ± 0.013

X-ray Photoelectron Spectroscopy (XPS)

Table S4. Atomic composition of the exfoliated samples as determined by XPS survey scans.

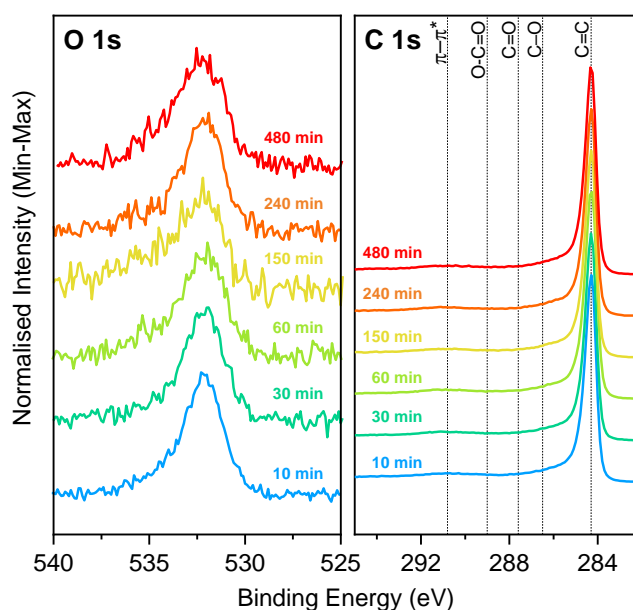| Sample ID	Atomic Composition / at%					O/C ratio
	C ±10 %	O ±20 %	Si ±100 %	Al ±100 %	Fe ±100 %	
10 min	96.7	2.4	0.6	0.2	0.1	0.025 ± 0.006
30 min	98.2	1.3	0.3	0.1	0.0	0.014 ± 0.003
60 min	98.3	1.3	0.3	0.1	0.0	0.013 ± 0.003
150 min	98.5	1.1	0.2	0.1	0.0	0.011 ± 0.003
240 min	98.1	1.4	0.3	0.2	0.0	0.015 ± 0.003
480 min	98.0	1.5	0.3	0.1	0.0	0.015 ± 0.004

Figure S9. Normalised high-resolution spectra of the O 1s and C 1s core levels acquired from the sonicated graphitic samples.

References

(1) Turner, P.; Hodnett, M.; Dorey, R.; Carey, J. D. Controlled Sonication as a Route to In-Situ Graphene Flake Size Control. *Sci. Rep.*, 2019, **9** (1), 1–8. https://doi.org/10.1038/s41598-019-45059-5.

(2) Kouroupis-Agalou, K.; Liscio, A.; Treossi, E.; Ortolani, L.; Morandi, V.; Pugno, N. M.; Palermo, V. Fragmentation and Exfoliation of 2-Dimensional Materials: A Statistical Approach. *Nanoscale*, 2014, **6** (11), 5926–5933. https://doi.org/10.1039/c3nr06919b.

(3) Whitaker, D. A.; Hayes, K. A Simple Algorithm for Despiking Raman Spectra. *Chemom. Intell. Lab. Syst.*, 2018, **179**, 82–84. https://doi.org/10.1016/j.chemolab.2018.06.009.

(4) Marchesini, S.; Paton, K. R.; Brennan, B.; Turner, P.; Pollard, A. J. Using Nuclear Magnetic Resonance Proton Relaxation to Probe the Surface Chemistry of Carbon 2D Materials. *Nanoscale,* 2021,**13**, 6389-6393. https://doi.org/10.1039/D0NR08937K